Classification
Physics Abstracts
82.70 — 87.20 — 68.00

Thermally induced budding of phospholipid vesicles — a discontinuous process

J. Käs ([1]), E. Sackmann ([1]), R. Podgornik ([2]), S. Svetina ([2, 3]) and B. Žekš ([2, 3])

([1]) Physik Department (Biophysik E22), Technische Universität München, James-Franck Strasse, D-8046 Garching, Germany
([2]) Department of Theoretical Physics (F-1), J. Stefan Institute, Jamova 39, 61111 Ljubljana, Slovenia
([3]) Institute of Biophysics, Medical Faculty, University of Ljubljana, Lipičeva 2, 61105 Ljubljana, Slovenia

(*Received 6 July 1992, revised 10 February 1993, accepted 11 February 1993*)

Abstract. — The process of thermally induced budding is studied for DMPC vesicles. With increasing temperature a pear shaped vesicle changes discontinuously into a pair of spherical vesicles connected by a narrow neck. In the course of the cooling process a thermal hysteresis in a stepwise manner is observed. The size of the daughter vesicle diminishes by repeated widening and narrowing of the neck until it finally remains open and the vesicle attains the pear shape again. These experimental findings are difficult to rationalize within the bare bilayer couple model of phospholipid vesicles. To model the discontinuous behavior in the heating process the expansion of the elastic energy of the bilayer up to the third order in the area difference of the two monolayers is empirically introduced. The van der Waals forces between mother and daughter vesicles are shown to be responsible for the repeated widening and narrowing of the neck in the cooling process.

1. Introduction.

It is well known that the shape of a closed phospholipid vesicle is determined by minimization of the elastic bending energy of its membrane [1-6]. There are two models for the appropriate energy. Both assume that the membrane is laterally incompressible and therefore its area cannot be changed and that also the volume compressibility is negligible and therefore the vesicle volume is constant. The spontaneous curvature model [1, 2] does not take explicitly into account the structure of the phospholipid membrane, which is composed of two monolayers, but implicitly allows for an asymmetric composition of the two monolayers, which leads to a spontaneous curvature. The relative stretching of the two monolayers, i.e. such changes of the areas of the two monolayers which conserve the average area, is allowed within this model and costs no energy. On the other hand, the bilayer couple model [3-6] assumes a symmetric membrane and therefore zero spontaneous curvature, but explicitly takes into account the membrane structure by requiring constant areas of the two monolayers [7, 8],

which means not only constant membrane area but also constant monolayer area difference. These two models are the two limiting cases of a general model which includes spontaneous curvature of the membrane as well as the bilayer couple concept [9-11].

For single component vesicles the membrane is symmetric, the spontaneous curvature is equal to zero and the bilayer couple model seems to be convenient to describe their shape. One therefore minimizes the bending energy

$$W_b = \frac{1}{2} k_c \int (c_1 + c_2)^2 \, dA \, . \tag{1}$$

Here k_c is the membrane bending elastic constant, while c_1 and c_2 are the principal curvatures of the membrane and the integration goes over the whole area of the neutral surface. Minimization is to be carried out at fixed values of vesicle volume V, area of the bilayer neutral surface A and difference between the areas of the two monolayers (ΔA).

The expression for the membrane bending energy (Eq. (1)) is scale invariant, i.e. for a given shape it does not depend on the vesicle size. It is therefore appropriate to choose the unit of length in such a way that the membrane area equals unity, i.e. in units of the radius of the sphere (R_s) with the membrane area A

$$R_s = \left(\frac{A}{4\pi} \right)^{\frac{1}{2}} . \tag{2}$$

It is also convenient to define the relative volume

$$v = \frac{V}{V_s}, \qquad V_s = \frac{4\pi R_s^3}{3} \tag{3}$$

and the relative difference between the areas of the two monolayers

$$\Delta a = \frac{\Delta A}{\Delta A_s}, \qquad A_s = 8\pi h R_s \tag{4}$$

while the relative area $a = 1$. In equation (4) h is the distance between the neutral surfaces of the two monolayers.

It is clear that the result of the minimization procedure does not depend on the value of the membrane bending constant and it is also appropriate to measure the membrane bending energy relative to the bending energy of the sphere

$$w_b = \frac{W_b}{8\pi k_c} . \tag{5}$$

It can be seen that the equilibrium shapes and the corresponding energies (w_b) depend only on the relative volume v and relative area difference Δa [6].

The above minimization procedure is usually performed for axially symmetric vesicles and gives all possible shapes and the corresponding membrane bending energies for any set of values of relative volume v and relative monolayer area difference Δa. A more compact form of presenting the results is to introduce classes of shapes. A class of shapes contains all the shapes which can be obtained in a continuous way if v and Δa are continuously changed. Each class of shapes exists only within a certain part of the $v/\Delta a$ phase diagram, which is limited by limiting shapes.

It has been recently shown [12] that because of the thermal expansion of the monolayers

temperature changes lead to sequences of shapes which can be described fairly well by the bilayer couple model. Depending on the pretreatment of the initial spherical vesicle, several types of shape sequences can be obtained with increasing temperature [13]. The main three possibilities for the vesicles of dimyristoyl phosphatidylcholine (DMPC) are :

- budding transitions leading to the formation of a spherical daughter vesicle attached by a narrow neck to a spherical mother vesicle ;
- discocyte-stomatocyte transitions leading to an inside budded vesicle and to an internal spherical daughter vesicle attached by a narrow neck to the spherical mother vesicle ;
- reentrant dumbbell-pear-dumbbell transitions.

It has been found [13] that in the first two cases the transitions to the final shapes are discontinuous. By increasing the temperature continuously, the shape changes continuously up to a temperature where the shape becomes unstable and without further temperature change transforms relatively fast into the final mother-daughter shape. In the cooling cycle the shape does not follow the same sequence of changes but the size of the daughter vesicle diminishes by repeated opening and closing of the neck, until it finally remains open and the vesicle attains the initial shape again.

Such discontinuous transitions cannot be described by the bilayer couple model. Namely, it can be easily shown [12, 13] that one obtains in the simplest case temperature changes of the relative volume v and the relative area difference Δa as

$$\frac{\mathrm{d}v}{\mathrm{d}T} = -\frac{3}{2}\beta v\,, \qquad \frac{\mathrm{d}\,\Delta a}{\mathrm{d}T} = \frac{3}{2}\beta\,\Delta a\,. \tag{6}$$

Here β is the thermal area expansivity. Therefore, a monotonous change of temperature leads to a monotonous change of the control parameters v and Δa and should lead to continuous shape changes, because the final shape (i.e. mother-daughter pair) belongs to the same class as the intermediate pear shapes. The variation of the volume with temperature can be neglected.

In sections 2 and 3 we shall present a detailed analysis of the budding transition for DMPC vesicles together with the shape changes in the cooling run. In section 4 we shall first show that the bilayer couple model cannot describe the observed discontinuous transition and the corresponding hysteresis. We shall then extend the bilayer couple model by allowing relative stretching of the two monolayers. Also this extended version of the bilayer couple model, which incorporates some features of the spontaneous curvature model, cannot account for the observed discontinuous behavior. It is the inclusion of the third order terms in the monolayer area difference into the elastic energy that makes the predictions to conform with the experiment for the heating run. Repeated opening and closing of the neck in the course of the cooling run can be explained by invoking so far [14] unrecognized contribution to the energy of a budding vesicle. It has its origin in the van der Waals interactions between the spherical mother and daughter vesicles. The estimated magnitude of these interactions, which are comparable to the membrane stretching energies, shows that they should be included into shape equilibrium considerations for a budding vesicle.

2. Experimental methods.

All experiments are performed with DMPC (dimyristoyl phosphatidylcholine) obtained from Avanti (Birmingham, AL) in water purified by a Millipore-system. A detailed description of the method to obtain giant vesicles is already given in reference [13]. The shape transitions are induced by temperature changes which cause a change in the area of the vesicle at constant volume. The vesicles were observed in a measuring chamber which is nearly free of thermal convection and which is already described in reference [13]. Each experiment consists of two

separate heating and cooling runs. The first heating and cooling run was performed continuously at a rate of about 0.01 °C/s. In this run the principal path of shape transitions occurring during the heating and recooling of the vesicle was observed and recorded with a Sony U-matic videorecorder. In the second cycle the stability of the shapes was determined by first heating and then cooling in steps of 0.1 °C. After each step the vesicle was observed for 15 min to check whether the shape is stable.

In order to control changes in surface area and volume constancy, the area and the volume of the vesicle were measured by image processing. For this purpose we used a real time frame grabber (Pixel Pipeline, Perceptics, Knoxville, TE, USA) in a Macintosh IIfx. The image processing software is based on the public domain program Image. To evaluate the volume and the area, the coordinates of the contour line of the vesicle were determined first and then the two main axes of the vesicle shape. To determine the main axes one first determines the center of gravity of the vesicle shape and then chooses the largest diameter as the first axis. The second axis is chosen perpendicularly to the first. The traced contour line and the two axes were then displayed on the video screen. During the experiment one moves the focal plane through the shape thus deciding which of the two axes is to be the rotational axis of the vesicle. Perpendicular to the rotational axis, the vesicle was divided into slices of one-pixel thickness. Adding up the volumes of the slices yielded the vesicle volume and summing up their circumferences the surface area. The volume was measured with an accuracy of 4.5 % and the area with an accuracy of 3 %. The measurements show that within the experimental accuracy the vesicle volume is temperature independent, while the membrane area increases linearly with temperature. The thermal area expansivity coefficient $\beta = \frac{1}{A}\frac{dA}{dT}$ is equal to $6.5 \times 10^{-3}\,K^{-1}$.

3. Experimental results.

Figure 1 shows a typical budding transition of the vesicle. Heating a spherical vesicle (not shown), which was kept under lateral tension at 24.5 °C for some time, the vesicle first becomes an oblate ellipsoid and then discontinuously transforms into a prolate ellipsoid and then continuously into a pear. Here we analyze the last part of this heating process, which is presented in figure 1, showing that stable pear shapes exist for temperatures smaller or equal to 40.8 °C. A further increase in temperature by 0.1 °C to 40.9 °C causes a first order transition to an outside budded state. This means that the pear shapes become unstable leading to the formation of a daughter vesicle connected to the mother vesicle by a narrow neck. The observed sequence of shape changes does not depend much on the heating rate and displays for faster, continuous heating at a rate of 0.01 °C/s the same behavior as the one shown in figure 1.

The thermal hysteresis of the vesicle of figure 1 during recooling is shown in figure 2. Starting at 41.0 °C the neck between the bleb and the mother vesicle is repeatedly widening and narrowing at 38.7 °C as well as at the three lower temperatures, 37.2 °C, 35.5 °C and 32.4 °C. The shapes with the open neck are unstable. At each widening and narrowing the radius of the daughter vesicle gets smaller and the radius of the mother vesicle increases. After each closing the vesicle pair fluctuates and only after an additional temperature decrease lateral tension develops in the membrane leading to a suppression of fluctuations. At 25.3 °C the neck finally opens and a stable pear shape is obtained again. This temperature is much lower than the temperature, at which the pear shape becomes unstable in the heating process, and the thermal hysteresis amounts to 19.6 °C, but the system is reversible in a sense that heating leads again to the sequence of shape changes as shown in figure 1.

The cooling process is different for slow cooling rate. If the vesicle is cooled from 41 °C in

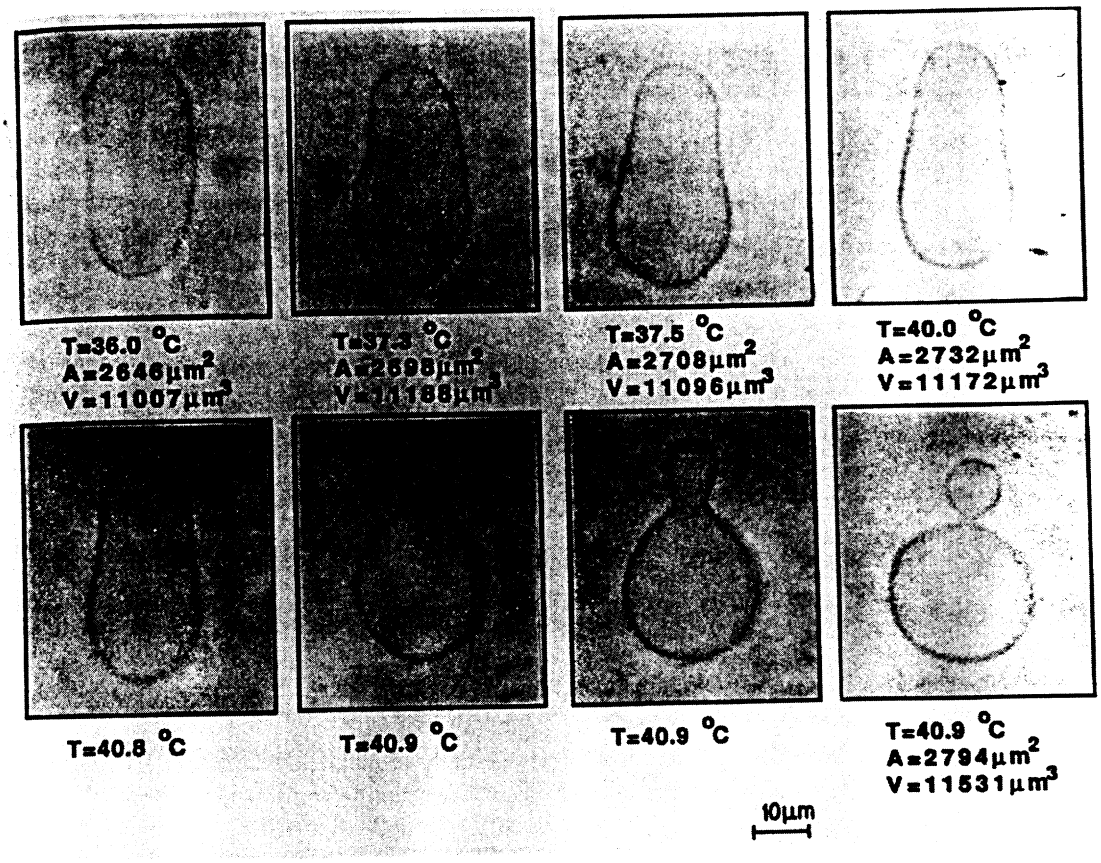

Fig. 1. — Typical budding transition of a DMPC vesicle in pure water. The shape transitions were induced by heating in steps of 0.1 °C. After each heating step the vesicle was observed for 15 min to prove the stability of the shape. The temperatures (T) and the measured volumes (V) and areas (A) are indicated in the pictures above. All the shapes for $T \leq 40.8$ °C are stable. The values of V and A at $T = 40.8$ °C cannot be determined because of large fluctuations of the shape. A further increase in temperature to 40.9 °C causes a spontaneous transition to an outside budded shape. This transition takes around 50 s. The first two pictures at 40.9 °C are showing instable, intermediate states. In the last picture at 40.9 °C the final outside budded shape is reached. It should be remarked that this final shape flickers.

steps of 0.1 °C with 15 min intervals, again repeated opening and closing of the neck is observed, but now at temperatures 39.7 °C, 31.6 °C, 28.5 °C and 26.4 °C, which means that the temperature intervals between two consecutive openings and closings increase. The vesicle now never transforms back into a pear shape. The neck remains closed till the temperature is lowered below the DMPC phase transition temperature (i.e. 23.8 °C) and the fission of the daughter vesicle occurs.

4. Theory.

4.1 BILAYER COUPLE MODEL. — As the basis for the interpretation of the presented series of vesicle shape changes we choose the systematics of the bilayer couple model. Within this model the vesicle shape can be determined by minimizing the membrane bending energy

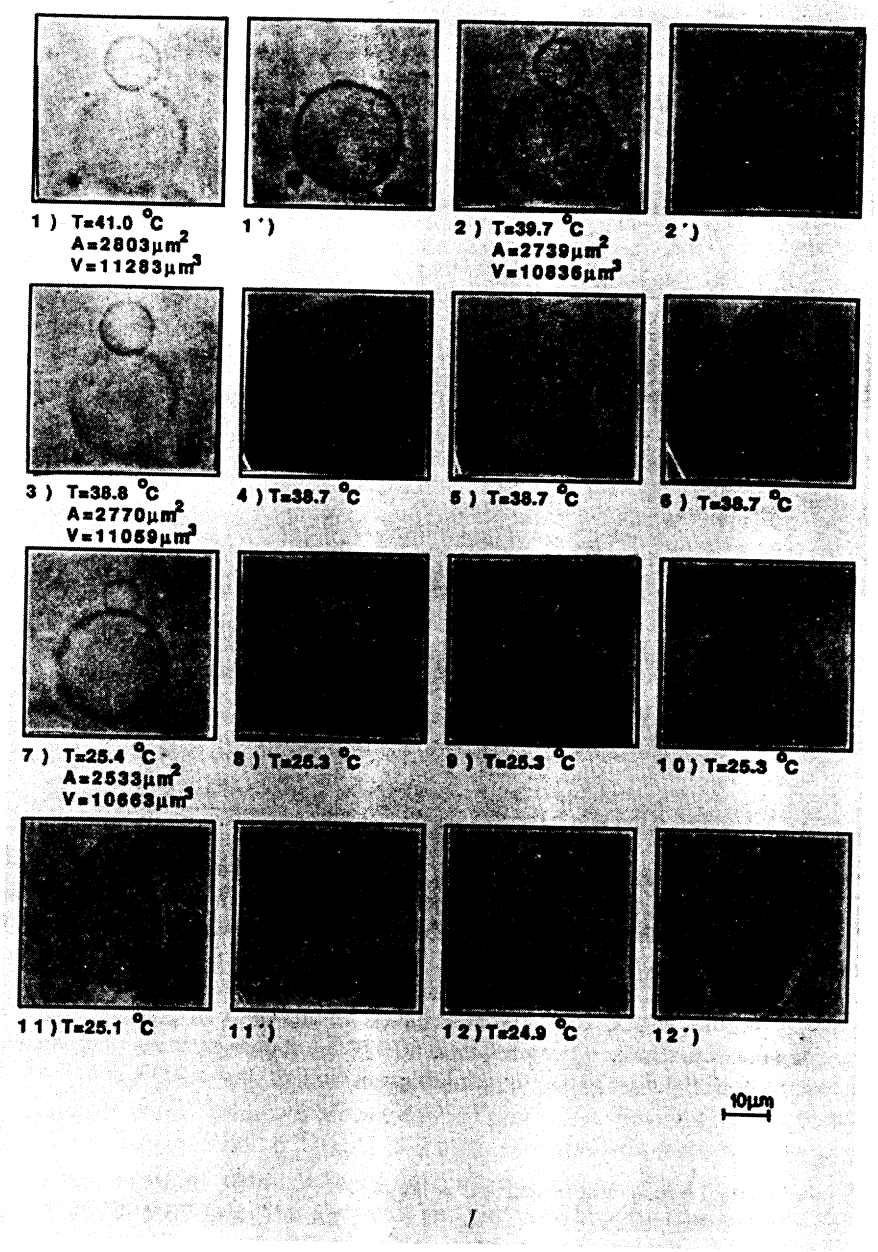

Fig. 2. — Transitions caused by recooling the budded vesicles of the figure 1. The cooling was performed continuously at a rate of 0.02 °C/s. The values for the temperature, T, the area A of the vesicle and the volume, V, of the vesicle are noted in the micrographs above. Pictures with the same number, dashed and undashed, as for e.g. 1 and 1′ are showing different focus planes of the same vesicle shape. During the cooling the neck between the mother and the daughter vesicle opens transiently at 38.7 °C (pictures 3, 4, 5, 6), 37.2 °C, 35.5 °C and 33.1 °C. The final opening of the neck occurred at 25.3 °C (pictures 7, 8, 9, 10). Before the opening of the neck the vesicle is always exposed to lateral stress. For e.g. before the neck opens at 38.7 °C the vesicle stops flickering at 39.7 °C, which means that a lateral tension exists in the membrane. Each opening and closing lasts for 10-20 s, while for the final opening 50 s are needed.

W_b (Eq. (1)) at constant vesicle volume and constant areas of the two membrane layers. The detailed analysis of the system [6] showed that the shapes obtained can be ascribed to different classes of shapes, where a class of shapes is defined to contain the shapes of the same symmetry which can be obtained in a continuous way by continuously changing relative volume v and relative area difference Δa.

The shapes described in the experimental section and in figures 1 and 2 belong to the class of axisymmetrical prolate ellipsoidal shapes with equatorial mirror symmetry (cigar class) and to the class of pear shapes. Figure 3 shows the relevant part of the vesicle shape $v/\Delta a$ phase diagram obtained by minimization of the bending energy (Eq. (1)). $v/\Delta a$ values for some of the shapes shown in figures 1 and 2 are marked. The relative volume v is determined from the measured values for vesicle volume and membrane area, and Δa is estimated by comparing the measured contours with the calculated series of shapes as the one shown for $v = 0.85$ in figure 4. Because of the small changes in v it makes perfect sense to treat v as essentially a constant quantity. The corresponding energy dependence is presented in figure 5. This presentation of data (Fig. 3) reflects the observation that shapes are changing continuously until a discontinuous transition to a limiting shape. Figure 3 also demonstrates that the hysteresis of the phenomenon of shape changes obtained by heating and cooling can be considered to be the hysteresis in the corresponding Δa and/or v values.

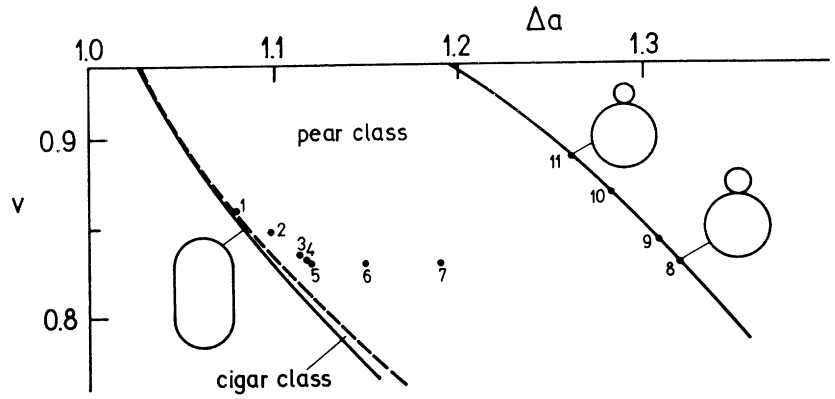

Fig. 3. — A part of relative volume/relative area difference vesicle shape phase diagram which is relevant for shapes described in the experimental section. The region of pear shapes is bounded on the left side by a broken line at which bilayer couple model predicts [15] a continuous transition from the shapes with the equatorial mirror symmetry (cigar shapes) to pear shapes. On the right side the pear shape region is bounded by the line connecting the limiting shapes which for the class of pear shapes are compositions of two linked spheres of different radii. The cigar shape region is bounded on the left side by a line of limiting shapes which are cylinders with spherical caps. Some of the calculated limiting shapes are also shown. Points denoted by 1-8 give v and Δa values corresponding to the eight shapes in figure 1, while only three points (points 9-11) corresponding to the limiting shapes obtained in the cooling run are shown, the one (point 11) with the largest relative volume corresponding to the shape before the final opening of the neck.

Thus, as already stated in the introduction (Sect. 1), the described observations do not seem to be consistent with predictions of the bilayer couple model because within this model discontinuous shape changes are not expected within one class for continuous changes of the control parameters v and Δa. As shown in figure 5, the bending energy is a monotonously increasing function of Δa and a monotonously decreasing function of v. Because the

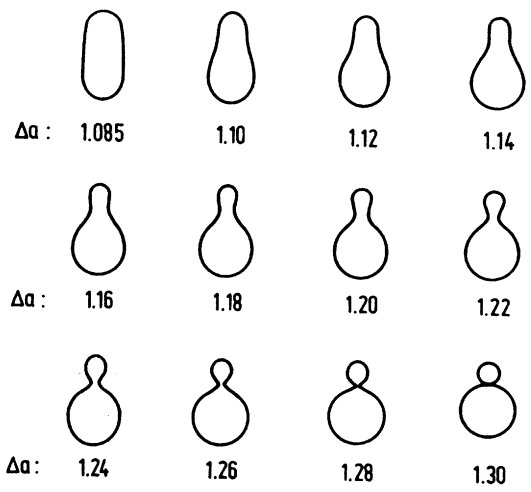

Fig. 4. — A series of shapes of the pear class DMPC vesicles with different values of the relative area difference Δa are shown for the relative volume $v = 0.85$.

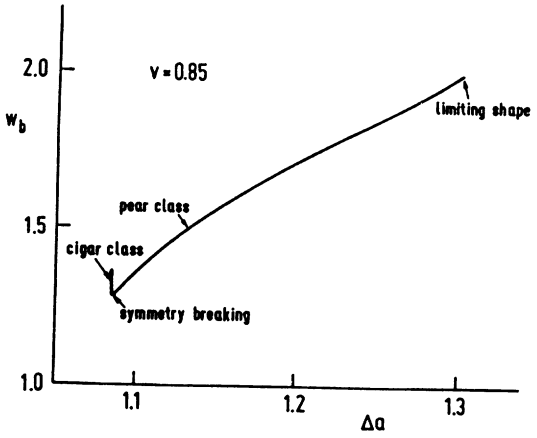

Fig. 5. — Dependence of the membrane bending energy (in units of 8 πk_c) on relative difference between the areas of the two layers (Δa) for the relative volume $v = 0.85$. It is seen that the dependence of the membrane bending energy for pear shapes on Δa is a monotonously increasing function. It can be shown that this dependence is steeper at higher relative volumes. Bending energy has its largest value ($w_b = 2$) at the limiting shapes.

experiments are done at temperatures well above the gel to liquid crystal phase transition temperature of DMPC ($T_c = 23.8$ °C) it can be assumed that the temperature changes of the relative volume and relative area difference are continuous.

4.2 RELATIVE STRETCHING AND SPONTANEOUS CURVATURE. — A possible extension of the bilayer couple model which could allow for discontinuous shape transitions is to include the relative expansivity of the two membrane layers into the analysis [9-11]. The shape of the vesicle is then determined by minimizing the sum of the bending energy w_b and the energy due to relative area expansivities w_r, which can be equivalently expressed as the non-local bending

energy of the membrane :

$$w^{(2)} = w_b + w_r . \tag{7}$$

The relative area expansivity term is also normalized with respect to the bending energy of a sphere ($8\pi k_c$) and can be expressed as

$$w_r = q(\Delta a - \Delta a_0)^2 \tag{8}$$

with q, the ratio between the non-local and local bending moduli [10, 11], and Δa_0 the relative area difference for the non-expanded membrane layers. The original bilayer couple model is obtained in the limit $q \to \infty$, while in the spontaneous curvature model $q = 0$. Recent measurements [11] gave an estimate for q to be in between 1 and 10.

It should be noted at this point that the inclusion of the relative stretching energy makes Δa_0 temperature dependent because of the thermal expansion whereas Δa attains a value which minimizes the total energy. Continuous changes in Δa_0 could therefore lead to discontinuous changes in Δa.

In order to illustrate the effect of the relative expansivity term, figure 6 shows, for $v = 0.85$, the dependence of the sum of the membrane bending and relative expansivity terms as a function of Δa, for different values of Δa_0 and for the value of the parameter $q = 10$. For this value of the parameter q the minimum of $w^{(2)}$ and corresponding stable pear shapes exist within the interval $1.13 < \Delta a < 1.30$. This example shows that the proposed extension of the bilayer couple model predicts a possibility of a discontinuous transition from a cigar type shape to a pear type shape (cf. $\Delta a_0 = 1.325$ curve in Fig. 6). Such a transition occurs

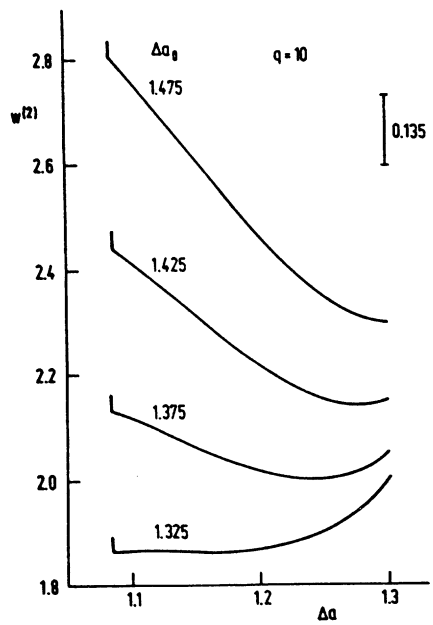

Fig. 6. — The sum of the membrane local and non-local bending energies as a function of the area difference Δa for the cigar and pear class shapes is plotted for different values of Δa_0 ($v = 0.85$). The ratio between the non-local and local bending moduli is chosen to be $q = 10$. A typical van der Waals binding energy (its exact value being dependent on the size of the mother and daughter vesicle) of the two vesicles ($w_{vdW} = 0.135$) is represented by a vertical line and should be subtracted from the elastic energy of a mother-daughter pair.

for values of q smaller than 20 which is the value of $\frac{dw_b}{d\Delta a}$ at the symmetry breaking point (Fig. 5). The smaller q the higher is the Δa value of the attained stable pear shape. For sufficiently small values of q the discontinuous transition leads actually to a nearly limiting shape. However, this transition starts from a shape with the equatorial mirror symmetry whereas the observations indicate that the transition is from a shape belonging to the class of pear shapes. The predicted shape transitions within the pear class are continuous which means that also on the basis of the model including the relative expansivity term it is not possible to interpret the discontinuous shape transitions obtained in the experiment (Fig. 1).

In a generalized model also the spontaneous curvature c_0 should be included in the bending energy that has to be described by [1, 16]

$$w_b = \frac{1}{2} k_c \int (c_1 + c_2 - c_0)^2 \, dA \, . \tag{9}$$

However, the inclusion of the spontaneous curvature does not change the behavior of the system with respect to predicted discontinuous transitions. Even more, « it leaves little or no room for a continuous budding transition through weakly asymmetric stable vesicle shapes such as eggs and pears » [16]. Thus within this energy expression (Eqs. (7) and (9)) even the fact that such pear transition states have been found experimentally appears to be puzzling.

The above analysis indicates that neither the bilayer couple model, nor the spontaneous curvature model or the combination of the two can describe the observed discontinuous transitions of the DMPC vesicles. Therefore in the following we consider two possible further interpretations of the experimental data. The first takes into consideration van der Waals forces between the two vesicle parts of the limiting shape and the second is based on the inclusion of third order terms in the elastic energy of the bilayers.

4.3 VAN DER WAALS FORCES. — One distinct line of approach to the problem would be to add the contribution of intravesicular forces to the elastic free energy of the system and analyse the shapes of the surface satisfying the minimization condition in such a generalized model. This has indeed been done by Bruinsma [17] in his study of growth instabilities of vesicles. Also Wortis *et al.* [14] suggested that such a term could be included in the analysis of lipid bilayer vesicles shapes including vesiculation and different shape transitions. The contribution of the intravesicular forces to the total free energy is shape dependent but since these forces have a very short range on the scale of the vesicle size their effects would be seen only in some limiting geometries. Thus the free energy due to the intravesicular forces would be small whenever the shape of the vesicle is such that its boundaries do not come into close proximity. Especially, for the budding transition this would mean that one has to take into account the intravesicular forces only in the last stages of the transition where two separate vesicles form in close proximity. Limiting ourselves to this blebbed state let us for the sake of the argument take two vesicles of radii R_1 and R_2 at a (minimal) separation L, connected with a thin neck. Since the sign of the total free energy (see Ref. [17]), $W(L)$, is negative we can refer to $W(L)$ as the binding energy of the blebbed vesicle. For plausible values of R_1, $R_2 \sim 10$ μm and $L \sim 20$ Å we can convince ourselves that the free energy of the neck is negligible compared to the contribution of the van der Waals interactions between the two (mother and daughter) vesicles. Nevertheless the neck itself is very important, because it keeps the mother and the daughter vesicle in close contact. We note that the above conclusions would remain valid also for binding energies derived from more general types of force laws that include forces with a range smaller than the van der Waals force [18].

The force curves for the interaction of planar membranes can be turned *via* the Derjaguin

approximation into interaction energies between spherical vesicles as has been done by Lis *et al.* [19]. The Derjaguin approximation [20] simply relates the interaction potential per unit surface area, $E(L)$, of two planar surfaces at the separation L to the force acting between two vesicles $F(L)$ at a (minimal) separation L

$$F(L) = 2\pi \left(\frac{R_1 R_2}{R_1 + R_2} \right) E(L) \quad \text{if} \quad R_1, R_2 \gg L \tag{10}$$

where R_1 and R_2 are the radii of the two spherical vesicles. The forces (or for that matter the free energy $W(L)$ that is the integral of the force) thus scale as $\left(\frac{R_1 R_2}{R_1 + R_2} \right)$. Thus we are in position to relate the binding energy $W(L)$ of a system of two spherical vesicles to the integral of the interaction potential between two flat membranes. For the region of L where van der Waals interactions dominate we can derive

$$W_{vdW}(L) \sim \left(\frac{R_1 R_2}{R_1 + R_2} \right) \frac{0.2\, kT}{L} \tag{11}$$

for the hydrocarbon over water planar geometry [20].

We now apply this reasoning to DMPC vesicles. The result of the measurements of Lis *et al.* [19] on flat DMPC membranes turned into a binding energy of two spherical vesicles of equal diameters (300 Å) at an equilibrium separation (giving a lower bound for the interaction energy) of 25 Å leads to a binding energy of approximately 0.3 kT. This value can now be translated *via* the R_1, R_2 scaling ratio in the Derjaguin approximation into a statement that two spherical vesicles of radii 13.3 and 6.7 μm (actually seen in the experiments) have a binding energy of approximately 90 kT at the same (minimal) separation.

This binding energy would thus have to be subtracted from the elastic energy in the blebbed state to obtain the total free energy of the system. Measuring the energy in elastic units of $8\pi k_c$, where $k_c = 1 \times 10^{-19}$ J, the value corresponding to the binding energy of 90 kT is $w_{vdW} = 0.135$. Taking into account the variation of the radii of the two blebs obtained in the experiment one is thus led to the following upper and lower bounds for the binding energy at a (minimal) separation of $L = 25$ Å in the blebbed state

R_1 [μm]	R_2 [μm]	$W_{vdW}(kT)$	w_{vdW}
13.3	6.7	90	0.135
13.5	4.4	68	0.101

As explained above we are only able to obtain the van der Waals energy for a shape, where two separate blebs are connected by a thin neck. This is not really a major drawback since the van der Waals energy is by far the largest at this particular point. On the phase diagram its contribution to the total free energy of the system would thus show as a single point at the end of the free energy line leading to a very sharp energy minimum for the limiting shapes. The estimated magnitude of the van der Waals binding energy w_{vdW} is shown as a vertical line in figure 6. This value, which is comparable to the changes in elastic energies should be subtracted from the energy of the limiting shape.

Though the inclusion of the van der Waals interactions between the mother and the daughter vesicles does lead to the lowering of the total energy of the budded state, some unsatisfactory

features have to be pointed out. The inclusion of the van der Waals energy leads in the dependence of the vesicle energy on Δa (Fig. 6) to the appearance of the two minima with a maximum in between. The transition should thus occur across an energy barrier and be therefore of the first order character. As the barrier height is very large ($> \simeq 50\, kT$), a very long relaxation time and a pronounced hysteresis can be expected for this transition. The observed instability corresponds to the case, when the vesicle in the heating process stays in a metastable pear state until the barrier decreases almost to zero and the pear shape simply destabilizes and transforms into the stable limiting shape. The van der Waals interactions cannot describe such an instability (Fig. 6), but nevertheless their magnitude is clearly within the range of energies governing the budding process and should be in one form or another included in any realistic model of this phenomenon.

4.4 THIRD ORDER TERMS IN THE ELASTIC ENERGY. — The elastic energy of a bilayer up to the third order in the monolayer area difference is introduced here without invoking any specific physical mechanism. In a most general form it can be written as

$$w^{(3)} = w_b(\Delta a) - c_0(\Delta a - \Delta a_0) + q(\Delta a - \Delta a_0)^2 - \frac{\gamma}{6}(\Delta a - \Delta a_0)^3 \qquad (12)$$

where $w_b(\Delta a)$ and the second order term have already been introduced and correspond to the bare elastic energy (Eq. (5)) and the relative stretching of the two membrane layers (Eq. (8)). The first order term is nothing but the spontaneous curvature term [1, 16] and thus the first three terms in the above energy expression contain all the contributions that have been taken into account into energy considerations up till now. The last term is the third order term and its consequences on the behavior of the energy in the budding process will be investigated below.

Within a small range of values of the parameters c_0, q and γ the total energy has a dependence on Δa_0 that would correspond to the observed discontinuous transition from a pear shape to the nearly limiting shape of the pear class shapes. This is shown in figure 7 where the total energy is plotted as a function of Δa for a consecutive set of Δa_0 values.

The phase diagram of the budding process (Fig. 7) now clearly exhibits all the features of the observed discontinuous transition. A single extremely steep minimum at the leftmost side of the energy curve for smaller values of Δa_0 (i.e. at low temperatures) is being first of all replaced by a somewhat broader minimum, that is slowly displaced towards larger values of the equilibrium Δa for larger values of Δa_0 (i.e. for higher temperature). At a certain value of Δa_0 (lying between 1.202 and 1.203) the equilibrium state of the system is discontinuously moved to the other minimum on the right side of the energy curve. This transition is effected without any crossing of an intervening energy barrier and thus closely conforms to the experiment. In the cooling run the vesicle must cross the potential barrier to transform back into a pear shape and therefore the thermal hysteresis appears.

The effect of van der Waals forces on the energy dependences in figure 7 is the same as the one presented in figure 6. They decrease the energy of the limiting shape and lead to a sharp minimum at maximal Δa.

4.5 THE BILAYER STRETCHING ELASTIC ENERGY. — In the cooling process the repeated opening and closing of the neck of the mother-daughter vesicle pair is observed. After each closing of the neck, the shape first fluctuates but after some additional temperature decrease the fluctuations are suppressed by the lateral stress which develops in the membrane. This can be understood by assuming that because of the van der Waals attraction the neck is closed for the water transport and for lipid diffusion between the daughter and mother vesicle. With decreasing temperature the membrane area would decrease — but at constant volume and with the closed neck it can not — and would thus lead to its stretching. The stretching and the

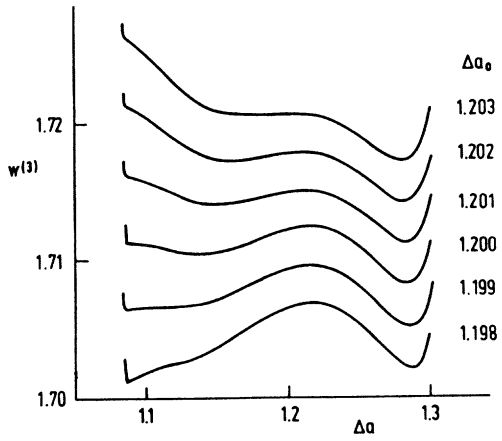

Fig. 7. — The elastic energy of the bilayer expanded up to the third order in $(\Delta a - \Delta a_0)$ for the pear class of shapes is plotted for different values of Δa_0, while v is kept constant ($v = 0.85$). The values of the parameters are $c_0 = 2.8$, $q = 3.4$ and $\gamma = 220$.

corresponding elastic energy increase with decreasing temperature until the stretching energy becomes comparable to the van der Waals energy of the neck. Then the neck opens transiently and the system equilibrates in a new mother-daughter pair with unstretched membrane.

As the typical temperature difference ΔT between the two consecutive openings and closings is for the fast cooling process of the order of one degree, $\Delta T \approx 1$ K, and the thermal area expansivity coefficient $\beta = 6.5 \times 10^{-3}\,\mathrm{K}^{-1}$, the corresponding fractional area dilation (α) is thus

$$\alpha = \beta\, \Delta T = 6.5 \times 10^{-3}\,. \tag{13}$$

This maximal area dilation is so small [21] that the membrane is always in the low tension regime, where its elastic properties are dominated by fluctuations and the relation between α and the membrane tension τ can be expressed as [22]

$$\alpha \approx \frac{kT}{8\,\pi k_c} \ln\left(1 + \frac{\tau A}{\pi^2 k_c}\right). \tag{14}$$

From this relation the increase of the elastic free energy can be evaluated as

$$W_{el} = A \int_0^{\alpha} \tau\, \mathrm{d}\alpha = \pi^2 k_c \left[\frac{kT}{8\,\pi k_c}\left(\mathrm{e}^{\frac{8\,\pi k_c}{kT}\alpha} - 1\right) - \alpha\right]. \tag{15}$$

Now the question can be asked, what temperature decrease ΔT is needed for an elastic energy W_{el} to become equal to the van der Waals binding energy (W_{vdW}). Taking for this the estimate $W_{vdW} = 0.135 \times 8\,\pi k_c$ and using the values $k_c = 1 \times 10^{-19}$ J and $A = 2\,800\ \mu\mathrm{m}^2$, one obtains from equation (15) and equation (13) $\Delta T = 1.3$ °C, which agrees well with measurements.

It must be remembered that the ΔT intervals get larger, if the cooling process is slower. This could mean that a very slow relaxation process exists and the neck is on such a long time scale not completely closed for the exchange of water and lipids. Because of this also the elastic free energy W_{el} is smaller and not big enough to allow the crossing of the energy barrier back to the

pear shape state. This increases the thermal hysteresis which becomes so large, that the membrane phase transition occurs before the vesicle transforms back into a pear shape.

5. Discussion and conclusions.

Attempts to understand the salient features of the budding processes in vesicles have already been presented (see e.g. Ref. [16]). There are, however, important novel distinctions brought forth by our work that can be summarized in two main conclusions.

First of all the (van der Waals) interactions between the mother and the daughter vesicles give a remarkable energy contribution to the total energy of the system whose magnitude is comparable to the magnitude of all the other energy changes involved in the budding process. This is something worth bearing in mind, since even if the van der Waals interactions are not driving the budding transition, their presence is an indispensable stabilizing factor acting in parallel with other mechanisms. The role of van der Waals forces is particularly important in the cooling process, where they are closing the neck and blocking the exchange of water and lipids between the two vesicles. Therefore a tension develops in the membrane, which finally opens the neck.

The major drawback to the idea that the van der Waals forces alone could drive the budding transition comes from the realization that in this case the system would have to overcome an interposed local energy maximum. One does not see this in the experiment. It was thus necessary to recognize that though the van der Waals interactions are important for the budding process they can not account for its driving mechanism. We tried to model it by an empirical energy expansion in terms of the relative area difference between the two constitutive layers of the membrane. It is shown that an inclusion of the cubic term in $\Delta a - \Delta a_0$ can describe the observed instabilities. The addition of the van der Waals contribution to the total energy only additionally stabilizes the budded state.

If the role of the van der Waals interactions is important in the budding process, then this fact in itself should have predictable consequences. First of all their importance should not depend on whether the vesicle shape would correspond to outside or inside budded states. The influence of the van der Waals interaction should also favour the budding of large vesicles and multilamellar vesicles because in these cases the energy minimum of the budded states should be deeper. We did not yet investigate this conclusion. The van der Waals forces thus appear to, if not directly to drive the budding transition, to at least have a very important role in its stabilization.

Finally we should recall a statement from the introduction that the type of the shape transition depends on the pretreatment. This could be explained by Δa_0, which takes into account a different number of phospholipids in the two monolayers. For example, if a spherical vesicle is exposed to lateral stress before a heating cycle, it shows a budding transition. The lateral stress causes an increase in the lipid flip flop rate and facilitates the equilibration of lipids and the change of Δa_0. A different initial value of Δa_0 means also that in the heating process $\Delta a_0(T)$ will behave differently.

References

[1] HELFRICH W., *Z. Naturforsch.* **28c** (1973) 693.
[2] DEULING H. J. and HELFRICH W., *J. Phys. France* **37** (1976) 1335.
[3] SVETINA S., OTTOVA-LEITMANNOVA A. and GLASER R., *J. Theor. Biol.* **94** (1982) 13.
[4] SVETINA S. and ŽEKŠ B., *Bio.ned. Biochim. Acta* **42** (1985) S86.
[5] SVETINA S., BRUMEN M. and ŽEKŠ B., *Stud. Biophys.* **110** (1985) 177.

[6] SVETINA S. and ŽEKŠ B., *Eur. Biophys. J.* **17** (1989) 101.
[7] EVANS E. A., *Biophys. J.* **14** (1974) 923.
[8] SHEETZ M. P. and SINGER S. J., *Proc. Natl. Acad. Sci. USA* **71** (1974) 4457.
[9] SEIFERT U., MIAO L., DÖBEREINER H.-G. and WORTIS M., The Structure and Conformation of Amphiphilic Membranes, R. Lipowsky, D. Richter and K. Kremer Eds. (Springer-Verlag, Berlin Heidelberg 1992) p. 93.
[10] BOŽIČ B., SVETINA S., ŽEKŠ B. and WAUGH R. E., *Biophys. J.* **61** (1992) 963.
[11] WAUGH R. E., SONG J., SVETINA S. and ŽEKŠ B., *Biophys. J.* **61** (1992) 974.
[12] BERNDL K., KÄS J., LIPOWSKY R., SACKMANN E. and SEIFERT U., *Europhys. Lett.* **13** (1990) 659.
[13] KÄS J. and SACKMANN E., *Biophys. J.* **60** (1991) 825.
[14] WORTIS M., SEIFERT U., BERNDL K., FOURCADE B., MIAO L., RAO M. and ZIA R. K. P., Proceedings of the workshop on « Dynamical Phenomena at Interfaces, Surfaces and Membranes », Les Houches, 18.2-28.2.1991, D. Beysens, N. Boccara and G. Forgacs Eds. (1991).
[15] SVETINA S. and ŽEKŠ B., *J. Theor. Biol.* **146** (1990) 115.
[16] WIESE W., HARBICH W. and HELFRICH W., *J. Phys. : Condens. Matter* **4** (1992) 1647.
[17] BRUINSMA R., *J. Phys. Colloq. France* **51** (1990) C7-53.
[18] RAND R. P., *Ann. Rev. Biophys. Bioeng.* **10** (1981) 277.
[19] LIS L. J., MCALISTER M., FULLER N., RAND R. P. and PARSEGIAN V. A., *Biophys. J.* **37** (1982) 657.
[20] ISRAELACHVILI J., Intermolecular and surface forces (Academic Press, New York, 1985).
[21] EVANS E. and RAWICZ W., *Phys. Rev. Lett.* **64** (1990) 2094.
[22] HELFRICH W. and SERVUSS R.-M., *Nuovo Cimento* **D3** (1984) 137.